Quantum Semiclass. Opt. 7 (1995) 601–613. Printed in the UK

# Quantum noise of free-running and externally-stabilized laser diodes

T-C Zhang†§, J-Ph Poizat†, P Grelu†, J-F Roch†, P Grangier†, F Marin‡, A Bramati‡, V Jost‡, M D Levenson‡|| and E Giacobino‡

† Institut d'Optique, BP 147, F91403 Orsay Cedex, France
‡ Laboratoire Kastler Brossel, Université Pierre et Marie Curie, F-75252 Paris Cedex 05, France

**Abstract.** We have investigated the intensity and phase noise of single-mode laser diodes, either free-running or using different types of line narrowing techniques at room temperature, namely feedback from an external grating and injection locking. We have measured an intensity squeezing of 1.2 dB in the first case, and 1.4 dB in the second case (respectively, 1.6 dB and 2.3 dB inferred at the laser output). We have observed that the intensity noise of a free-running 'single-mode' laser diode actually results from a cancellation effect between large anticorrelated fluctuations of the main mode and of weak longitudinal side modes. It is also shown that free-running diodes exhibit very large excess phase noise, typically more than 80 dB above shot noise at 10 MHz, which can be significantly reduced by the above-mentioned techniques.

## 1. Introduction

Quantum noise reduction in laser emission based on pump-noise suppression was first predicted in 1984 [1]. Semiconductor lasers are particularly well suited for the implementation of this property since it is possible to drive them with a current whose noise is well below shot noise. If the quantum efficiency of the carrier-to-photon conversion is high enough, the electron statistics of the pumping can be transferred to the light emission, yielding sub-Poissonian operation of the laser. Quantum noise in the intensity of constant-current-driven laser diodes was observed for the first time by Machida *et al* in 1987 [2], and further improved to 8.3 dB in 1991 [3]. This result was obtained in a measurement at 4 K, where the detector was closely coupled to the laser. The difficulties encountered by other groups in reproducing this result suggested that factors other than the constant current supply could be important for the noise reduction. In 1993, it was shown by Steel and his group [4, 5] that line-narrowing techniques (cf [6] and references therein) greatly helped in the noise reduction by further suppressing the weak but very noisy longitudinal side modes. Intensity squeezing of 3 dB (4.3 dB if corrected for detection efficiency) at 10 K and of 1.8 dB (2.0 dB corrected) at room temperature was obtained by injection locking the laser [5] or by feedback from an external grating [4], respectively.

We have investigated intensity noise but also more generally quadrature noise of laser diodes, using various methods for line narrowing, including injection-locking with another diode laser or a Ti:Sapphire laser, and feedback from an external grating. The best intensity squeezing at room temperature was 1.4 dB (2.3 dB when corrected for the detection efficiency), and was obtained with injection-locking. As far as quadrature noise is concerned,

§ Institute of optoelectronics, Shanxi University, Taiyuan 030006, China.
|| Levenson Consulting, 19868 Bonnie Ridge Way, Saratoga CA 95070, USA.

1355-5111/95/040601+13$19.50 

we have shown that the large excess phase noise of semiconductor lasers can be partially reduced by these line-narrowing techniques.

## 2. Experimental set-up. General features

The laser diodes we have used are index-guided quantum well GaAlAs laser diodes (model SDL 5422-H1 and SDL 5411-G1), operating at 850 and 810 nm. The rear facet reflection coefficient is 95%, the front facet is AR coated with a reflection coefficient of about 4%. The laser diodes are temperature stabilized and carefully electromagnetically shielded. Appropriate electrical filtering is used on the power supply†. The free-running laser diodes have a rather low threshold of 18 mA and a differential quantum efficiency (slope above threshold) of 66%. The operating current in the experiments described below is typically 5–7 times larger than the threshold current, and the resulting high overall quantum efficiency is at the origin of the squeezing. No squeezing was found in similar experiments performed on laser diodes with higher threshold (80 mA), which operate only 2 times above their threshold.

The quantum noise in the intensity is measured in the standard way with balanced detection [7]. The beam going out of the laser is split in two equal parts by a beamsplitter. Each output of the beamsplitter is sent into a high efficiency (90%) photodiode (EG&G model FND100 or C30809E). The DC parts of the photodiode currents are filtered out while the AC parts are amplified using 20 MHz bandwidth amplifiers. The amplifiers' outputs, proportional to the noise signals, are either subtracted or added by a RF $+/-$ power combiner. When set on the difference position, the circuit gives a signal proportional to the shot noise, while in the sum position, it gives the full intensity noise of the beam impinging on the beamsplitter. The output of the $+/-$ power combiner is sent to a spectrum analyser and noise spectra are recorded for the sum and the difference signals. The electronic noise is then substracted on each recording.

Consistency between the shot noise of a laser diode measured in this way and the noise of a white light source was carefully checked. The beamsplitter is either a 50/50 coated plate or a polarizing beamsplitter preceded by a half-wave plate. In the latter case, a polarizer must be placed at the output of the laser diode, in order to eliminate the small component of polarization perpendicular to the main polarization direction [5, 8]. Otherwise, the interference between the two components, which are mixed by the polarizing beamsplitter, may give rise to errors in the noise measurements.

When biased with a high voltage ($V > 70$ V), the photodiodes do not exhibit any DC saturation, for detected powers up to at least 45 mW. The AC response has a slight linear dependence on the detected DC power. However, the response is the same for the sum and difference positions of the power combiner, and so the balanced detection is not affected by the change in the AC response. At high powers, heating of the photodiodes causes a small decrease in the noise signal when the detectors have been illuminated for a few tens of seconds. In such cases, noise measurements were performed using short time intervals. Finally, consistency checks for high values of detected power were done by measuring the noise reduction as a function of the value of a neutral density filter, inserted in the beam before the photodiodes.

Two types of set-ups were investigated to achieve line narrowing: cavity extension with an external grating and injection-locking with another laser.

† We have used RC filters ($R = 47\ \Omega$, $C = 1\ \mu$F) for a driving current less than 100 mA, and $LC$ filters ($L = 1\ m$H, $C = 1\ \mu$F) for higher currents.

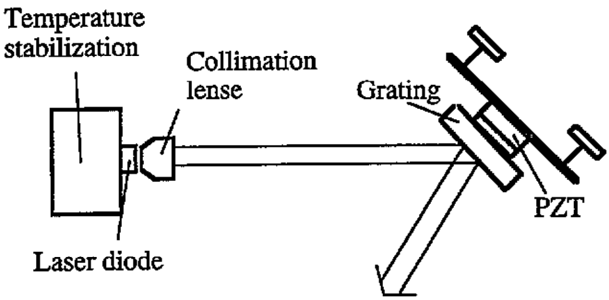


**Figure 1.** External grating stabilization scheme.

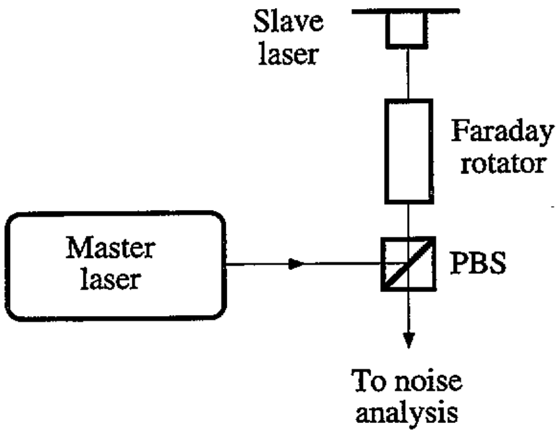


**Figure 2.** Injection-locking scheme. The Faraday rotator rotates the linear polarization by 45°, PBS is a polarizing beam splitter. The master laser is either a grating-extented laser diode (cf figure 1) or a frequency stabilized Ti:Sapphire laser.

The extended-cavity laser diode is shown in figure 1. The beam going out of the laser diode is collimated with a $f = 8$ mm objective placed in front of the output facet of the diode. The cavity is extended to 10 cm with a reflection holographic grating (Jobin–Yvon, 1200 lines/mm) reflecting the first order into the cavity, while the zero order goes out of the cavity (Littrow configuration). The grating is glued on a piezoelectric transducer, which is mounted on a finely orientable mirror mount. The efficiency of the grating is 60% in the zero order (output coupling) and 24% in the first order (feedback to the laser), with 16% losses. The alignment of the grating is critical. When it is achieved, the threshold of the laser is lowered from 18–13 mA and the DC power of the side modes goes down to −60 dB below the DC power of the main mode, while the total intensity noise is decreased below the shot-noise level.

The injection-locking scheme is depicted in figure 2. The master laser is either an external-grating diode laser or a Ti:Sapphire laser. It is injected into the slave laser by means of an optical isolator. The master beam enters through the escape port of the polarizer placed after the Faraday rotator. Locking is observed over a rather broad power range† of the master laser, from 1–4 mW. The direction of the master laser must be carefully adjusted for optimum noise reduction.

The detection scheme for the quadrature noise measurement is described in the corresponding section (section 4).

† It should be mentioned that only a small fraction (a few per cent) of this injected power is actually coupled to the lasing mode of the diode due to the imperfect mode overlap.

## 3. Intensity squeezing

### 3.1. Experimental results

We have investigated intensity squeezing in the two cases described above. Noise spectra were recorded for various supply currents. Squeezing was observed for currents higher than 50 mA ($I/I_{th} = 2.8$) for the injected laser and 30 mA ($I/I_{th} = 2.4$) for the extended cavity laser, at noise frequencies from 1–30 MHz (limited by our detection bandwidth). The noise, measured with a resolution bandwidth of 1 MHz, was nearly constant from 7–30 MHz. The optimum squeezing was observed in the injection-locking scheme. At 7 MHz, with a driving current of 130 mA, we obtained a noise reduction of 27%, i.e. 1.4 dB. Taking into account the total detection quantum efficiency of 65% from the laser output power to the photodiode current (through the optical isolator), we infer a value of 2.3 dB at the output of the laser diode. The best squeezing obtained with the grating-extended cavity is 25% (1.2 dB) at 30 MHz and 110 mA, from which we infer a 1.6 dB noise reduction at the output of the

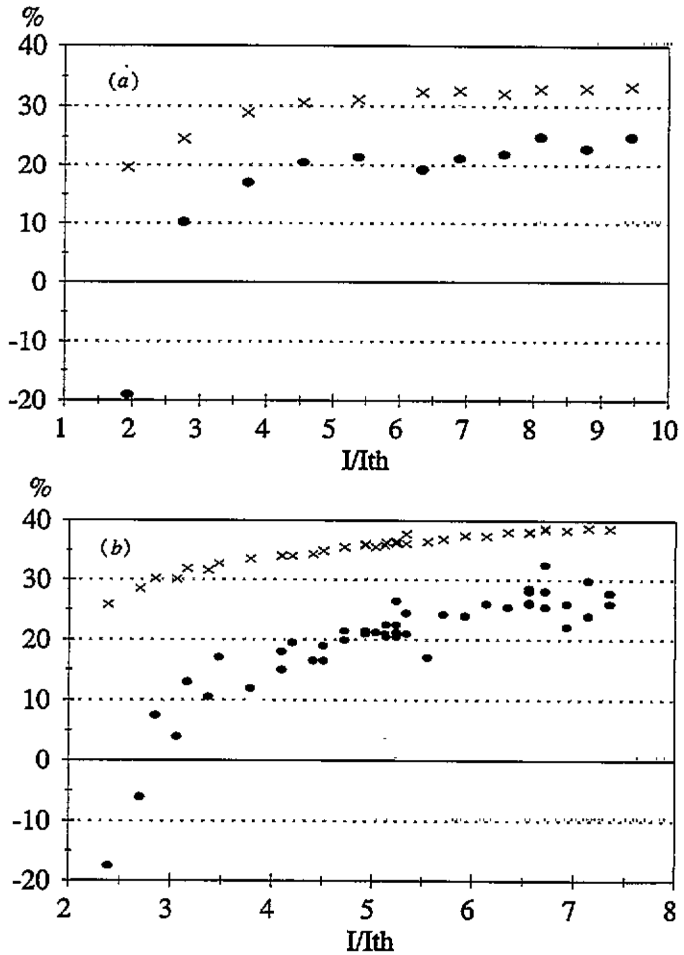


**Figure 3.** Noise reduction (full circles) and ratio of the detector current to the driving current (crosses) versus driving current normalized to threshold, (*a*) for the grating and (*b*) injection-locked.

grating. The fact that the squeezing is better with the injection-locking scheme can be attributed to the large losses due to the grating.

These numbers are close to those of [4, 5]. They are below the theoretical maxima expected from the quantum efficiency of the laser, which are, respectively, 58% (3.8 dB) at 130 mA for the injected laser and 42% (2.4 dB) at 110 mA for the grating-extended cavity. To check the dependence of the noise reduction on the laser diode quantum efficiency, in figure 3 we have plotted the intensity squeezing and the ratio of the detector current to the driving current against the driving current for the grating-extended laser (figure 3($a$)) and for the injection-locked laser (figure 3($b$)). It can be noticed that the ratio between the intensity squeezing and the current-to-current efficiency goes towards a maximum asymptotic value of 0.75, instead of the expected value of unity. Steel and coworkers, using similar laser diodes, obtained comparable values for this ratio: 0.83 for an injection-locked laser at 10 K [5] and 0.72 for a room temperature laser with external grating feedback [4]. This non-unity value can be attributed to additional noise sources in the semiconductor devices which are not included in the simple theoretical prediction mentioned above. Let us note that Richardson *et al* [3] observed a squeezing of 85% with a current-to-current efficiency of only 48%. This was attributed to the existence of another non-lasing junction, connected in parallel to the lasing one, and to the fact that 'electrical splitting' does not introduce partition noise [9, 10]. These various observations show that a comprehensive theoretical model of the quantum noise of laser diodes is still needed.

### 3.2. *Role of the longitudinal side modes*

The free-running laser diode apparently operates on a single mode. However, the longitudinal side modes have a non-negligible power, the closest ones being only −10 to −25 dB below the main mode (figure 4). The arguments given in [4, 5] to explain why

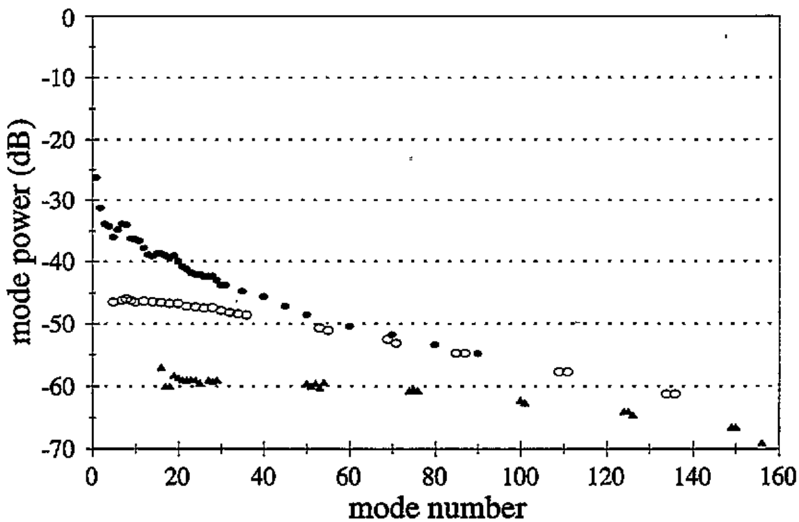


**Figure 4.** Power of individual longitudinal modes (optical power in dB, with respect to the main mode), measured with a high-resolution monochromator, for a driving current of 80 mA. On the $x$-axis each mode is labelled by a number, the number 0 corresponding to the main mode. The full circles are for the free-running laser, the open circles for the injection-locked laser, and the full triangles for the external grating configuration.

side-mode suppression reduces the total intensity noise to below the shot-noise level, tend to suggest that because these side modes are very noisy, the less powerful they are the less they will contribute to the total intensity noise. In order to explore these arguments more precisely, we have investigated the noise properties of individual modes by sending the laser beam through a high-resolution spectrometer. We have observed that the intensity noise of the main mode of a free-running laser diode is much larger (40 dB above shot noise) than the total intensity noise (2 dB above shot noise). This low value of the total intensity noise is then explained by very strong anticorrelations between the intensity noise of the main mode and the one of the whole set of side modes [11]. This effect will be analysed experimentally and theoretically in a forthcoming publication [12].

## 4. Phase noise

### *4.1. Quadrature noise detection scheme*

The investigation of the phase noise of a laser beam requires a phase-to-amplitude converter, i.e. a device whose complex transmission $T$ depends on the frequency $\omega$. In this paper, for this purpose we use the reflection off an empty detuned Fabry–Pérot cavity [13] as shown in figure 5. When the rear mirror is highly reflecting, this system has the advantage over a Mach–Zehnder interferometer that the mean-field transmission $|T(\omega = 0)|$ does not depend on the cavity detuning and is always equal to unity. This makes the shot-noise reference level independent of the quadrature analysed. Phase noise analysis is then carried out conveniently for frequencies in the range of the cavity bandwidth.

Explicit expressions of the quadrature rotation after reflection off a detuned Fabry–Pérot cavity are given in appendix A. A simple way to understand this effect is to have in mind that in Fourier space, the quadrature component $X(\omega)$ can be written as $X(\omega) = (a(\omega) + a^\dagger(\omega))/\sqrt{2} = (a(\omega) + [a(-\omega)]^\dagger)/\sqrt{2}$. The key point which yields a quadrature rotation is that the various frequency components at 0 (mean field), $\omega$ and $-\omega$ do not undergo the same phase shift when the laser is scanned across the resonance peak of the cavity. The quadrature rotation is zero in two cases: when the laser is tuned exactly

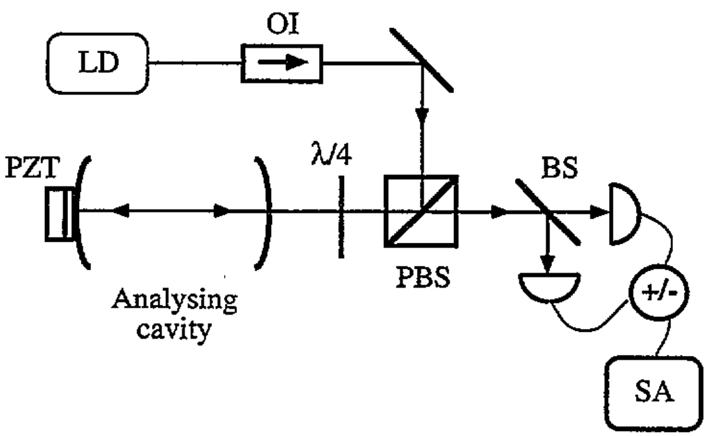


**Figure 5.** Phase noise detection set-up. Great care has been given in order to avoid any feedback from the analysing cavity to the laser, and optical isolation (OI) of about 80 dB has been used. The rear mirror is a high reflector and its position is controlled by a piezo electrical transducer (PZT).

on resonance, where the phase shifts for both frequency components $\pm\omega$ cancel out, and when it is tuned far outside the peak, where all frequency components undergo the same phase shift of 0 or $\pi$.

In our set-up the Fabry–Pérot cavity has a half-width at half-maximum (HWHM) of 8 MHz and a finesse of $\mathcal{F} = 125$. The rear mirror is highly reflecting, but its small leaks nevertheless allow us to monitor the intracavity intensity to adjust the mode matching. One of the mirrors is mounted on a piezo-electrical transducer, so that the length of the cavity can be scanned.

### *4.2. Experimental results*

We have measured the quadrature noise of a laser diode in the same three configurations which were used for the intensity noise measurements described above. These results are presented in figure 6. The phase noise (quadrature angle $\pi/2$ with respect to the mean field)

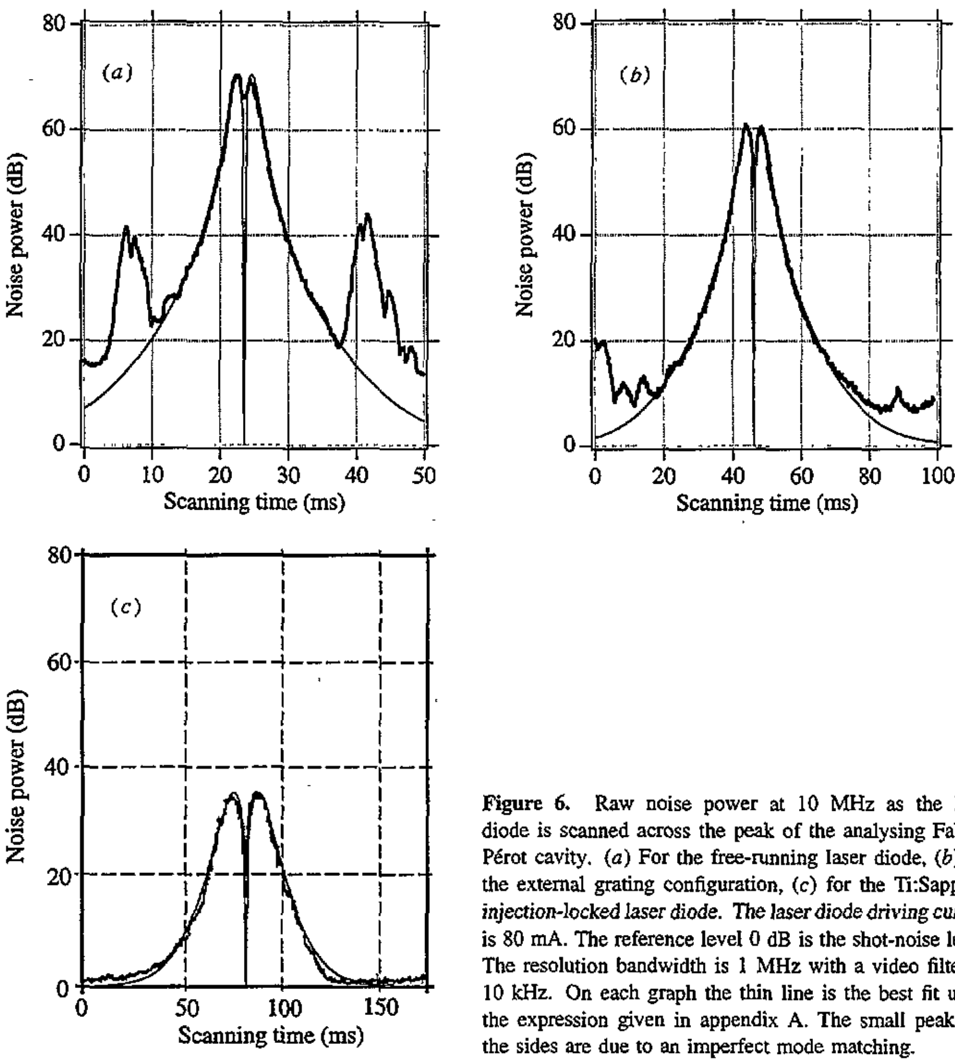


**Figure 6.** Raw noise power at 10 MHz as the laser diode is scanned across the peak of the analysing Fabry–Pérot cavity. (*a*) For the free-running laser diode, (*b*) for the external grating configuration, (*c*) for the Ti:Sapphire injection-locked laser diode. The laser diode driving current is 80 mA. The reference level 0 dB is the shot-noise level. The resolution bandwidth is 1 MHz with a video filter of 10 kHz. On each graph the thin line is the best fit using the expression given in appendix A. The small peaks on the sides are due to an imperfect mode matching.

is inferred from the experimental curves by fitting them with a simple model (see appendix A). This model has a single adjustable parameter which is the excess phase noise. This value has then to be corrected for various losses: propagation from the output of the laser to the detectors (3 dB), scattering losses inside the analysing cavity (3 dB on resonance), imperfect mode matching to the cavity (1 dB).

The phase noise inferred at the laser output for the free-running diode, the external grating configuration and the injection-locked scheme are of 82 dB, 72 dB and 46 dB, respectively, above the shot-noise level.

Let us compare these experimental results with the prediction given by the Schawlow–Townes model [14] (see appendix B). Within this model, the phase noise normalized to the shot-noise level at a noise angular frequency $\omega = 2\pi f$ is

$$V_\Phi(\omega) = 1 + \frac{8DI_o}{\omega^2}(1+\alpha^2) = 1 + \frac{2\kappa^2(1+\alpha^2)}{\omega^2} \tag{1}$$

where $I_o$ is the flow of photon outside of the laser (photons/sec), $\kappa$ is the cavity decay rate for intensity, $\alpha$ is the line enhancement factor [15] (also called the phase–amplitude coupling coefficient), and $D$ is the Schawlow–Townes phase diffusion coefficient defined in (B17). The first term is the contribution of the vacuum fluctuation (shot noise) and the second term is due to the phase diffusion assuming a random walk of the phase in the laser.

Using the value of $\kappa$ deduced from the experiment† one can calculate a theoretical estimation of the phase noise if the factor $(1+\alpha^2)$ is known. Conversely, by using the experimental value of the phase noise in (1), one can deduce a value of $(1+\alpha^2) = 10$, which is in agreement with other measurements. However, the linewidth of the laser diode was also measured directly by sending the light through a Fabry–Pérot cavity with a linewidth (HWHM) of 2 MHz. We obtained $D(1+\alpha^2)/(2\pi) = 2$ MHz (HWHM linewidth). Using the value $I_o = 2.5 \times 10^{17}$ photons/sec corresponding to 60 mW laser output, the above model predicts $D(1+\alpha^2)/(2\pi) = \kappa^2(1+\alpha^2)/(8\pi I_o) = 50$ kHz, which is significantly smaller than the measured value. This discrepancy could be attributed to jitter of the laser frequency due to power supply noise and thermal fluctuations.

In the injection locking case, the phase noise reduction mechanism relies on the fact that the slave laser locks its phase to that of the master laser [16]. The phase noise of this master laser is therefore of great importance. In this experiment we have used a frequency-stabilized Ti:Sapphire laser, which has a linewidth of 500 kHz and is both phase and intensity shot-noise limited at 10 MHz. We have observed a very significant phase noise reduction, from 82 to 46 dB for an injected power of 2 mW (see figure 6(*c*)).

Finally, let us emphasize that the quadrature noise detection scheme that we used is expected to work well only for a true single-mode laser. As was discussed previously (section 3.2), this is not the case for so-called 'single-mode' laser diodes, for which weak longitudinal side modes are very noisy and can therefore play an important role in the overall noise behaviour. As long as the intensity noise power in the main mode is small with respect to the total phase noise power, which is generally the case in the results described above, these effects can be neglected. However, one has to be cautious in some cases. For instance, it can be noticed that the experimental trace of figure 6(*c*) exhibits a slight asymmetry around its basis. This effect can be modelled simply with the equations of appendix A, using an input covariance matrix such that the main axis of the noise ellipse is not exactly the phase axis (quadrature angle $\pi/2$) but is slightly tilted. In our experiments,

† The quantity $1/\kappa$ is the lifetime of the photon in the laser diode cavity, calculated from the measured free spectral range of $\Delta\lambda = 0.12$ nm, and from the transmission coefficient of the output mirrors ($R_1 = 95\%$ and $R_2 = 4\%$). This yields $\kappa = (c\Delta\lambda/\lambda^2)\ln(1/(R_1R_2)) = 1.8 \times 10^{11}\ \mathrm{s}^{-1}$.

this small rotation effect has only been observed for the injection-locked laser, decreases as the driving current increases, and the dip on the right-hand side was always above the shot noise [17, 18]. It is likely that a detailed analysis of this effect should include the contributions of the small modes, since intensity–phase correlations are essential in this process.

## 5. Conclusions

In this paper we have reported on a detailed experimental analysis of both intensity and phase noise of commercial laser diodes at room temperature. We have studied the free-running diode and two other configurations using different line-narrowing techniques (injection-locking or external grating).

We have measured an intensity noise of 1.2 dB below the shot-noise level (1.6 dB inferred at the laser output) in the external grating configuration, and an intensity noise of 1.4 dB below shot noise (2.3 dB inferred at the laser output) for the injection-locked laser. Also, preliminary results show that these low-noise properties of quasi-single-mode laser diodes are actually due to cancellation of the large excess noise of the main mode by the anticorrelated noise of many weak but very noisy longitudinal side modes [12].

Concerning the measurements on quadrature noise, the main result is that laser diodes exhibit a very large excess phase noise (up to 80 dB above shot noise for the free-running laser), which can be partially decreased by line-narrowing techniques. The passive feedback from an external grating reduces the spectral width of the emitted light, thereby decreasing the phase noise from 82–72 dB above shot noise. In the injection-locking scheme, the phase noise reduction mechanism also involves the master laser, and using a shot-noise limited frequency stabilized Ti:Sapphire laser, we observed a reduction of the phase noise from 82 to 46 dB above shot noise.

We believe that these results have important practical implications for spectroscopy and quantum optics experiments involving laser diodes.

## Acknowledgments

This research was carried out within the framework of the ESPRIT Basic Research Project 6934 QUINTEC, and of the HCM network 'Non-Classical Light' (ERB CHRX CT93 0114). Two of us had fellowships: AB was supported by the HCM programme from the European Community (ERB CHBG CT93 0437), and TCZ was supported by the Programme International de Coopération scientifique (PICS) sponsored by the CNRS.

## Appendix A. Quadrature rotation after reflection on a detuned cavity

In this appendix we give the explicit input–output expression for the fluctuating amplitude and phase quadrature components at an analysis frequency $\omega$ (respectively, $\delta p^{in,out}(\omega)$ and $\delta q^{in,out}(\omega)$) of a field reflecting off a detuned cavity. We define

$$\delta c^{in,out}(\omega) = \begin{pmatrix} \delta p^{in,out} \\ \delta q^{in,out} \end{pmatrix}. \tag{A1}$$

We have then

$$\delta c^{out}(\omega) = R(\omega)\delta c^{in}(\omega) \tag{A2}$$

with

$$R_{11}(\omega) = R_{22}(\omega) = \frac{4\omega^2\kappa^2 + \kappa^4 - 16\omega^2\lambda^2 + 8\kappa^2\lambda^2 + 16\lambda^4}{\left(\kappa^2 + 4\lambda^2\right)\left(4\omega^2 - 4\mathrm{i}\,\omega\kappa - \kappa^2 - 4\lambda^2\right)}$$
$$R_{21}(\omega) = -R_{12}(\omega) = \frac{16\omega^2\kappa\lambda}{\left(\kappa^2 + 4\lambda^2\right)\left(4\omega^2 - 4\mathrm{i}\,\omega\kappa - \kappa^2 - 4\lambda^2\right)} \tag{A3}$$

where $\kappa$ is the cavity decay rate and $\lambda$ the cavity detuning.

The angle $\beta$ of the quadrature rotation is given by

$$\tan\beta = \frac{R_{12}(\omega)}{R_{11}(\omega)}. \tag{A4}$$

Let us now give the expression we used for the fits of figure 6, displaying the noise at a given analysis angular frequency $\omega$ of a laser light exhibiting an excess phase noise as the length of the cavity is scanned around a resonance peak. We define the input and output noise covariance matrix $V^{in}$, $V^{out}$ in the $p$, $q$ basis as

$$V^{in,out}(\omega) = \tfrac{1}{2}(V^{in,out}_{(+)} + V^{in,out}_{(-)}) \qquad \text{where} \qquad V^{in,out}_{(\pm)} = \delta c^{in,out}(\pm\omega)[\delta c^{in,out}(\mp\omega)]^T. \tag{A5}$$

These two matrices are then linked using (A2), and we obtain

$$V^{out}_{(\pm)}(\omega) = R(\pm\omega)V^{in}_{(\pm)}[R(\mp\omega)]^T. \tag{A6}$$

The quantity plotted in the fits of figure 6 is the coefficient $V^{out}_{11}$ versus the cavity detuning $\lambda$ at a given $\omega$. The input noise covariance matrix used for these plots is the one of a field whose amplitude noise is at the shot-noise level and whose phase noise is $v^{in}_q$ time above shot noise ($v^{in}_q$ is the adjustable parameter in the fits):

$$V^{in}(\omega) = \begin{pmatrix} 1 & 0 \\ 0 & v^{in}_q \end{pmatrix}. \tag{A7}$$

It can be mentioned that the use of non-zero off-diagonal elements for $V^{in}$ models the asymmetry resulting from a phase-amplitude coupling very well in the injection-locking case (figure 6($c$)).

## Appendix B. Link between phase noise, frequency noise and linewidth

In this appendix, we wish to recall some definitions and to present formulae linking together quantities used in the main part of the paper, such as phase and frequency noise spectra, and the linewidth of a single-mode laser.

In a semiclassical model, the slowly varying part of the electric field of a single-mode electromagnetic field can be written as

$$\alpha(t) = (I(t))^{1/2}\,\mathrm{e}^{\mathrm{i}(\phi_o + \phi(t))} \tag{B1}$$

where $I(t)$ is the (eventually fluctuating) intensity, $\phi_o$ is the phase origin, and $\phi(t)$ is a fluctuating phase with $\langle\phi(t)\rangle = 0$. In this expression, as everywhere else in the paper, the term $\mathrm{e}^{\mathrm{i}\omega_o t}$ oscillating at the optical frequency has been taken out, and $\omega = \omega_{opt} - \omega_o$ is a RF angular frequency. In the following, we will also consider only stationary random processes, and brackets will denote ensemble averaging (or time averaging, which is the same assuming ergodicity). The field variable $\alpha(t)$ will be considered as a $c$-number, but quantum noise can be readily included using standard techniques in quantum optics. If the $P$ representation (normal ordering) is used, the vacuum noise contribution in the correlation functions is zero, and shot noise has to be included using the standard theory of photodetection [20]. On the other hand, it is also possible to use the Wigner representation (symmetrical ordering), which directly includes vacuum noise contributions, and therefore shot noise effects in the spectra [21]. In the following, we will rather use normal ordering, and shot noise will appear only at the end of the calculation.

The phase noise power spectrum at $\omega = 2\pi f$, where $f$ is the RF noise analysis frequency, is given by

$$S_\phi(\omega) = (2\pi)^{-1/2} \int_{-\infty}^{\infty} \mathrm{e}^{\mathrm{i}\omega t} \langle \phi(t)\phi(0) \rangle \,\mathrm{d}t\,. \tag{B2}$$

On the other hand, the instantaneous angular frequency $\omega(t)$ is given by

$$\omega(t) = \frac{\mathrm{d}[\phi_o + \phi(t)]}{\mathrm{d}t} = \dot{\phi}(t) \tag{B3}$$

and therefore the frequency noise spectrum is given by

$$S_{\dot{\phi}}(\omega) = (2\pi)^{-1/2} \int_{-\infty}^{\infty} \mathrm{e}^{\mathrm{i}\omega t} \langle \dot{\phi}(t)\dot{\phi}(0) \rangle \,\mathrm{d}t\,. \tag{B4}$$

A simple calculation yields the well known formula

$$S_{\dot{\phi}}(\omega) = \omega^2 S_\phi(\omega)\,. \tag{B5}$$

Let us also define the quantity $\Delta_\tau\phi(t) = \phi(t+\tau) - \phi(t)$, whose noise spectrum is

$$S_{\Delta_\tau\phi}(\omega) = (2\pi)^{-1/2} \int_{-\infty}^{\infty} \mathrm{e}^{\mathrm{i}\omega t} \langle \Delta_\tau\phi(t)\Delta_\tau\phi(0) \rangle \,\mathrm{d}t\,. \tag{B6}$$

It is then straightforward to show that

$$S_{\Delta_\tau\phi}(\omega) = 2(1 - \cos\omega\tau) S_\phi(\omega)\,. \tag{B7}$$

The quantity $S_{\Delta_\tau\phi}(\omega)$ is useful in order to relate the quantities defined above to the spectral lineshape (one has $\omega = \omega_{opt} - \omega_o$, hence the lineshape is centred on zero instead of $\omega_o$):

$$L(\omega) = (2\pi)^{-1/2} \int_{-\infty}^{\infty} \mathrm{e}^{\mathrm{i}\omega\tau} \langle \alpha^*(\tau)\alpha(0) \rangle \,\mathrm{d}\tau\,. \tag{B8}$$

Assuming that the intensity noise is negligeable (i.e. that the orthoradial fluctuations of the Fresnel vector are much larger than the radial ones), and denoting $I_o$ the average intensity expressed in photons/sec, we have

$$\langle \alpha^*(t+\tau)\alpha(t) \rangle = I_o \langle \exp(-\mathrm{i}\Delta_\tau\phi(t)) \rangle\,. \tag{B9}$$

The imaginary part of $\langle \exp(\mathrm{i}\Delta_\tau\phi) \rangle$ vanishes for symmetry reasons. A standard assumption at this point is that $\Delta_\tau\phi$ is a stationary Gaussian random variable [19]. Its variance, which will be denoted by $\sigma_\tau^2$, is given by the integral of the spectrum

$$\sigma_\tau^2 = (2\pi)^{-1/2} \int_{-\infty}^{\infty} S_{\Delta_\tau\phi}(\omega) \,\mathrm{d}\omega\,. \tag{B10}$$

We can then write

$$\begin{aligned} \langle \alpha^*(\tau)\alpha(0) \rangle &= I_o\, (2\pi\sigma_\tau^2)^{-1/2} \int_{-\infty}^{\infty} \mathrm{e}^{\left(-\frac{(\Delta_\tau\phi)^2}{2\sigma_\tau^2}\right)} \cos(\Delta_\tau\phi)\, \mathrm{d}(\Delta_\tau\phi) \\ &= I_o\, \mathrm{e}^{\left(-\frac{\sigma_\tau^2}{2}\right)} \end{aligned} \tag{B11}$$

from which the expression of the spectral lineshape (B8) can be readily deduced.

In the case where $\Delta_\tau\phi(t)$ is generated by a random walk process, it is possible to derive analytical expressions for all these quantities. The fact that $\Delta_\tau\phi(t)$ is a random walk process means that the phase derivatives at different times are not correlated, i.e.

$$\forall t_1, t_2, \langle\dot{\phi}(t_1)\dot{\phi}(t_2)\rangle = 2\ D\ \delta(t_1 - t_2) \tag{B12}$$

where $D$ is a constant, and $\delta$ the Dirac function. The frequency noise spectrum (cf equation (B4)) is then given by

$$S_{\dot{\phi}}(\omega) = (2\pi)^{-1/2}\int_{-\infty}^{\infty} e^{i\omega t}2D\delta(t)\,dt = \frac{2D}{\sqrt{2\pi}} \tag{B13}$$

and is thus independent of $\omega$ (white frequency noise). Using equation (B5), the phase noise spectrum can be written

$$S_\phi(\omega) = \frac{1}{\sqrt{2\pi}}\frac{2D}{\omega^2}. \tag{B14}$$

Furthermore, it is a well known result [22] that the variance $\sigma_\tau^2$ of a random walk process is proportional to $\tau$, and it is easy to show, using (B7), (B5) and (B10), that

$$\sigma_\tau^2 = 2D|\tau|. \tag{B15}$$

The lineshape $L(\omega)$ can then be expressed explicitly, using its definition (B8) and (B11),

$$\begin{aligned} L(\omega) &= (2\pi)^{-1/2}\int_{-\infty}^{\infty} I_o e^{i\omega\tau}\, e^{-D|\tau|}\,d\tau \\ &= I_o\,\frac{D(2/\pi)^{1/2}}{D^2+\omega^2} \end{aligned} \tag{B16}$$

which is the usual Lorentzian shape of the laser linewidth (Schawlow–Townes formula [14]). Identifying equation (B16) with the Schawlow–Townes expression, we can relate the coefficient $D$ to the parameters of the laser which generated this light, and we have, for a laser far above threshold [21]:

$$2D = \frac{\kappa^2}{2I_o} \tag{B17}$$

where $\kappa$ is the laser cavity (intensity) decay rate.

As was said at the beginning of this appendix, these calculations have been done using normal ordering. The contribution of phase vacuum fluctuations (to the linewidth for example) is therefore zero, but the shot noise will appear in the detected phase noise power, calculated using the standard methods quoted at the beginning. We finally obtain the total phase noise power that would be read on a spectrum analyser at frequency $f = \omega/(2\pi)$:

$$\begin{aligned} V_\phi(\omega) &= S_\phi^{vac}(\omega) + S_\phi(\omega) \\ &= \frac{1}{\sqrt{2\pi}}\left(\frac{1}{4I_o} + \frac{2D}{\omega^2}\right) \\ &= \frac{1}{\sqrt{2\pi}}\frac{1}{4I_o}\left(1 + \frac{2\,\kappa^2}{\omega^2}\right). \end{aligned} \tag{B18}$$

At a given angular frequency $\omega$, the phase noise is therefore the sum of the shot noise and of a term proportional to the laser linewidth. In equation (1) of the text, this expression has been normalized to the shot-noise level, and the linewidth enhancement factor $(1+\alpha^2)$ has been added in the second term.

## References

[1] Golubev Yu M and Sokolov I V 1984 *Zh. Eksp. Teor. Phys.* **87** 804 (1984 *Sov. Phys.–JETP* **60** 234)
[2] Machida S, Yamamoto Y and Itaya Y 1987 *Phys. Rev. Lett.* **58** 1000
[3] Richardson W H, Machida S and Yamamoto Y 1991 *Phys. Rev. Lett.* **66** 2867
[4] Freeman M J, Wang H, Steel D G, Craig R and Scifres D R 1993 *Opt. Lett.* **18** 2141
[5] Wang H, Freeman M J and Steel D G 1993 *Phys. Rev. Lett.* **71** 3951
[6] Wieman C E and Hollberg L 1991 *Rev. Sci. Instrum.* **62** 1
[7] Yuen H P and Chan V W S 1983 *Opt. Lett.* **8** 177
[8] Freeman M J, Wang H, Steel D G, Craig R and Scifres D R 1993 *Opt. Lett.* **18** 379
[9] Edwards P J and Pollard G H 1993 *Phys. Rev. Lett.* **69** 1757
[10] Goobar E, Karlsson A, Björk G and Rigole P-J 1993 *Phys. Rev. Lett.* **70** 437
[11] Inoue S, Ohzu H, Machida S and Yamamoto Y 1992 *Phys. Rev.* A **46** 2757
[12] Marin F, Bramati A, Giacobino E, Zhang T-C, Poizat J-Ph, Roch J-F and Grangier P 1995 *Phys. Rev. Lett.* submitted
[13] Levenson M D, Shelby R M and Perlmutter S H 1985 *Opt. Lett.* **10** 514
Galatola P, Lugiato L A, Porreca M G, Tombesi P and Leuchs G 1991 *Opt. Commun.* **85** 95
[14] Schawlow A L and Townes C H 1958 *Phys. Rev.* **112** 1940
[15] Henry C H 1982 *IEEE J. Quantum Electron.* **18** 259
[16] Spano P, Piazzolla S and Tamburrini M 1985 *Opt. Lett.* **10** 556; 1986 *IEEE J. Quantum Electron.* **22** 427
[17] Kikuchi K, Watanabe K and Katoh K 1994 *Appl. Phys. Lett.* **65** 2533
[18] Karlsson A and Björk G 1991 *Phys. Rev.* A **44** 7669
[19] Daino B, Spano P, Tamburrini M and Piazzolla S 1983 *IEEE J. Quantum Electron.* **19** 266 and references therein
[20] Glauber R J 1965 *Ecole d'été des Houches* 1964 ed C de Witt, A Blandin and C Cohen-Tannoudji (Gordon and Breach)
[21] Courtois J Y, Smith A, Fabre C and Reynaud S 1991 *J. Mod. Opt.* **38** 177
[22] Papoulis A 1965 *Probability, Random Variables and Stochastic Processes* (New York: McGraw-Hill) p 290